

## ORIGINAL ARTICLE

## Cannabinoid CB1 receptors in distinct circuits of the extended amygdala determine fear responsiveness to unpredictable threat

MD Lange<sup>1,3</sup>, T Daldrup<sup>1,3</sup>, F Remmers<sup>2</sup>, HJ Sz kudlarek<sup>1</sup>, J Lesting<sup>1</sup>, S Guggenhuber<sup>2</sup>, S Ruehle<sup>2</sup>, K Jüngling<sup>1</sup>, T Seidenbecher<sup>1</sup>, B Lutz<sup>2</sup> and HC Pape<sup>1</sup>

The brain circuits underlying behavioral fear have been extensively studied over the last decades. Although the vast majority of experimental studies assess fear as a transient state of apprehension in response to a discrete threat, such phasic states of fear can shift to a sustained anxious apprehension, particularly in face of diffuse cues with unpredictable environmental contingencies. Unpredictability, in turn, is considered an important variable contributing to anxiety disorders. The networks of the extended amygdala have been suggested keys to the control of phasic and sustained states of fear, although the underlying synaptic pathways and mechanisms remain poorly understood. Here, we show that the endocannabinoid system acting in synaptic circuits of the extended amygdala can explain the fear response profile during exposure to unpredictable threat. Using fear training with predictable or unpredictable cues in mice, combined with local and cell-type-specific deficiency and rescue of cannabinoid type 1 (CB1) receptors, we found that presynaptic CB1 receptors on distinct amygdala projections to bed nucleus of the stria terminalis (BNST) are both necessary and sufficient for the shift from phasic to sustained fear in response to an unpredictable threat. These results thereby identify the causal role of a defined protein in a distinct brain pathway for the temporal development of a sustained state of anxious apprehension during unpredictability of environmental influences, reminiscent of anxiety symptoms in humans.

*Molecular Psychiatry* (2017) **22**, 1422–1430; doi:10.1038/mp.2016.156; published online 4 October 2016

## INTRODUCTION

Depending on the physical or psychological distance to threat, responsiveness of mammals can shift from a quickly developing and rapidly dissipating state of fear to a more long-lasting state of anxious apprehension that can turn into a pathological state if it becomes extreme.<sup>1–4</sup> Although decades of research have identified brain circuits and mechanisms mediating fear responses to a discrete threat in a good detail,<sup>5–9</sup> the central mechanisms shifting fear to anxiety states are less understood.<sup>10</sup> Operationalization of these states as phasic and sustained fear in response to predictable and unpredictable threat, respectively, provided important entry points to experimental studies in both humans and rodents.<sup>11–14</sup> Importantly, animals exposed to unpredictable but not to predictable threats show behaviors reminiscent of anxiety symptoms in humans,<sup>15,16</sup> emphasizing the role of unpredictability in anxiety disorders. Available data suggest that synaptic networks of the extended amygdala, involving central amygdala (CeA) and bed nucleus of stria terminalis (BNST), are keys to the control of these states.<sup>11,17</sup> A large body of evidence has favored the view that CeA is required for the rapid expression of phasic fear to discrete sensory cues,<sup>6,8</sup> functions that are left unaltered after BNST inactivation.<sup>11</sup> Lesions of BNST, in contrast, interfere with sustained components of fear.<sup>11,17,18</sup> Although functional subregions and types of neurons have been identified in basal amygdala (BA), CeA and BNST,<sup>8,19–24</sup> it remains elusive how the extended amygdala networks mediate the individual

response profiles to predictable *versus* unpredictable threat. This is an important issue, as many symptoms of clinical anxiety are better reflected in sustained rather than phasic fear paradigms.<sup>11</sup> The endocannabinoid (eCB) system is an attractive candidate for controlling states of fear and anxiety: it is known to regulate synaptic transmission in amygdala and BNST on demand,<sup>25–30</sup> and physiological responses to stress modulate the expression levels of its key components.<sup>31–34</sup> We have used genetic inactivation and rescue techniques to interfere with the eCB system in a cell-type- and pathway-specific manner. Combined with behavioral pharmacology and optogenetics/electrophysiology, we present evidence indicating that the eCB system, acting on presynaptic cannabinoid type 1 (CB1) receptors on distinct amygdala inputs to BNST, is both necessary and sufficient for the shift from phasic to sustained fear in response to an unpredictable threat.

## MATERIALS AND METHODS

## Animals

All animal experiments were carried out in accordance with European regulations on animal experimentation (Directive 2010/63/EU of the European Parliament and of the Council of 22 September 2010) and protocols were approved by the local authorities (Landesamt für Natur, Umwelt und Verbraucherschutz Nordrhein-Westfalen; reference number: 8.87-51.05.20.10.189). The study was performed on adult male mice

<sup>1</sup>Institute of Physiology I, Westfälische Wilhelms-University Münster, Münster, Germany and <sup>2</sup>Institute of Physiological Chemistry, University Medical Center of the Johannes Gutenberg-University Mainz, Mainz, Germany. Correspondence: Professor H-C Pape, Institute of Physiology I, Westfälische Wilhelms-University, Robert-Koch-Street 27A, Münster D-48149, Germany.

E-mail: papechris@ukmuenster.de

<sup>3</sup>These authors contributed equally to this work.

Received 19 February 2016; revised 20 July 2016; accepted 20 July 2016; published online 4 October 2016

(2–6 months old) of different lines (for mouse line details see Supplementary Material and Methods).

### Stereotaxic surgery and viral injection

Virus packaging and determination of titer were performed as previously described.<sup>35</sup> For surgery, animals were deeply anesthetized with i.p. injection of pentobarbital (50 mg kg<sup>-1</sup>) and s.c. injection of carprofen (4–5 mg kg<sup>-1</sup>; Rimadyl, Pfizer, Berlin, Germany). Stereotaxic surgery and viral injections were performed as described previously.<sup>36</sup> Viral injections were performed at the following stereotaxic coordinates: BA, coordinates from bregma: -1.6 mm anteroposterior (AP); ±3.3 mm mediolateral (ML); -3.9 mm dorsoventral (DV); CeA, AP: -1.6 mm; ML: ±3.0 mm; DV: -3.9 mm; MeA, AP: -1.6 mm; ML: ±2.5 mm; DV: -5 mm. A 10- $\mu$ l microsyringe (nanofil; WPI, Sarasota, FL, USA) was used to deliver AAV solution at a rate of 0.05  $\mu$ l min<sup>-1</sup> using a microsyringe pump (UMP3; WPI) and its controller (Micro4). Mice displaying spread of eYFP- or mCherry-fluorescence outside the target region were excluded. For details see Supplementary Material and Methods.

### Guide cannula implantation

For pharmacological intervention studies, guide cannulas (polyimide coated silica tubes; inner diameter (id): 250  $\mu$ m, outer diameter (od): 360  $\mu$ m; Polymicro Technologies, Phoenix, AZ, USA) were implanted bilaterally at the following stereotaxic coordinates: aBNST, coordinates from bregma: +0.15 mm AP; ±0.9 mm ML; -3.8 mm DV (for details see Supplementary Material and Methods).

### Electrophysiological recordings

Mice were anaesthetized with isoflurane (1-chloro-2,2,2-trifluoroethyl-difluoromethylether; 2.5% in O<sub>2</sub>; Abbott, Wiesbaden, Germany) and decapitated. Coronal slices (300  $\mu$ m thick) containing BNST were prepared. Whole-cell patch-clamp recordings (in voltage- or current-clamp mode) were performed as described previously.<sup>37</sup> For details see Supplementary Material and Methods. Gabazine (25  $\mu$ M), CGP55845 (10  $\mu$ M), D-(-)-2-amino-5-phosphonopentanoic acid (AP5, 50  $\mu$ M), and 6,7-dinitroquinoxaline-2,3-dione (DNQX, 10  $\mu$ M) were added to the bathing solution as required to block GABAergic or glutamatergic postsynaptic currents (PSCs).

### Postsynaptic responses evoked by light or electrical stimulations

Whole-cell recordings were obtained under voltage-clamp condition from single BNST neurons at holding potential of -60 mV. The intracellular solution contained 50  $\mu$ M Alexa-Fluor594 to visualize neuronal morphology. ChR2-containing fibers were readily visible by their eYFP-fluorescence. For light stimulation, GABAergic or glutamatergic transmission was evoked by scanning a small region around the dendrites (~12  $\mu$ m<sup>2</sup>) with 3.3 ± 1% of the maximal intensity of a 473 nm laser (scan time ~25 ms; LD473, Olympus, Tokyo, Japan; for details see Supplementary Figure S1 and Supplementary Material and Methods).

### DSE and DSI

For all depolarization-induced suppression of excitation (DSE) and inhibition (DSI) measurements, the stimulation strength was set to evoke ~50% of the maximal light- or electrically-induced PSC amplitude. DSE and DSI protocol consisted of 30 stimuli (at 0.2 Hz) applied as light stimuli of ChR2-containing fibers in BNST or electrical stimulation within the local BNST neuropil, and 90 of these stimuli after postsynaptic depolarization from -60 to 0 mV. The duration of depolarization was 10 s (for details see Supplementary Material and Methods).

### Immunohistochemistry

Immunohistochemistry was performed as described previously.<sup>27</sup> We used a polyclonal antibody against CB1 (rabbit anti-CB1; 1:500; ImmunoGenes, Budakeszi, Hungary; 1% NGS, 0.1% BSA, and 0.3% Triton X-100 in PBS). As a secondary antibody we used a Cy3-labeled goat anti-rabbit-IgG (1:250, Jackson ImmunoResearch, West Grove, PA, USA). Stained slices were analyzed with a laser scanning confocal microscope (Nikon eC1 plus, Nikon, Düsseldorf, Germany; for details see Supplementary Material and Methods).

### Behavioral analysis

Behavioral testing was performed using a fear training paradigm with either predictable or unpredictable pairings of conditioned (CS) and unconditioned (US) stimuli (Supplementary Figure S2).<sup>13,14</sup> In an adaptation session (day 1), 36 startle-eliciting white noise bursts (duration: 50 ms, inter-burst interval: 30 s) were presented to mice within the test cage. Fear conditioning (day 2) was performed within a standardized fear conditioning chamber (Fear Conditioning System, TSE, Bad Homburg, Germany). In two sessions, mice were presented with a total of eight 10 kHz tones (CS, 75 dB, unpredictable training: presentation with pseudo-randomized duration of 9, 14, 19 and 29 s, ISI 30 s; predictable training: constant duration of 10 s, pseudo-randomized ISI of 15, 19 and 20 s) and coinciding scrambled footshocks (US, 0.4 mA, 1 s). 24 h after fear conditioning (day 3), separate groups of vehicle- and pharmacologically treated C57BL/6J animals were tested for fear memory retrieval of predictable or unpredictable threat to distinguish between phasic and sustained components of conditioned fear. In all other animals that had received pharmacological treatment and/or viral injections, retrieval of fear was tested after unpredictable training. The retrieval and conditioning contexts differed in all experiments. Freezing (immobility except of respiratory movements) was evaluated by an experienced experimenter (naive to experimental conditions) using video file recordings and the keylogger-function of Spike2 software (version 7, CED, Cambridge, UK).

The pharmacological treatment and histological verification are described in detail in Supplementary Material and Methods.

### Data analysis and statistics

Data are presented as mean and standard error of the mean ( $\pm$  s.e.m.). *Ex vivo/in vitro*: Data were analyzed using repeated-measurement ANOVA (SPSS, IBM, Armonk, NY, USA) followed by Bonferroni *post hoc* test and one-sample *t*-test, respectively. Statistically significant outliers were identified and excluded from analysis by using Grubb's test (significance level  $P < 0.05$ ). The number of experiments is given as (no. of cells/no. of animals). *In vivo*: Freezing was scored in percent per 30 s time bins across experimental period using a customized MATLAB routine (MATLAB 7.11.0 (R2010b), The MathWorks, Natick, MA, USA). No statistical methods were used to predetermine sample size. Analysis of variance (ANOVA) with repeated measurements was used to analyze freezing behavior between groups followed by Bonferroni *post hoc* test for multiple comparisons. Experiments were performed in a randomized fashion.

## RESULTS

The BNST is a heterogeneous structure,<sup>19,23</sup> and intense CB1 immunolabeling has previously been detected in the anterior section of the rat BNST on putative GABAergic and glutamatergic terminals.<sup>38</sup> In the present study, immunohistochemical stainings in mice ( $N = 5$  animals) revealed fiber-like structures forming CB1 immunoreactive mesh-like pattern in the anterodorsal BNST (adBNST), with high levels in the anterolateral (aBNST) compared with low levels in the anteromedial (amBNST) section and oval BNST (ovBNST) (Figure 1a). To assess the functional significance of CB1 receptors, we used a fear training paradigm with predictable or unpredictable pairings of CS and US, where the unpredictability of threat results in a shift from transient phasic to more sustained fear (Supplementary Figure S2).<sup>13</sup> Vehicle-injected animals exposed to this paradigm shifted to a significantly prolonged and sustained freezing, lasting throughout the entire CS presentation, compared with rapidly declining phasic freezing in animals that were trained to predictable threat (Figure 1b; statistical data in Supplementary Table S1). Local bilateral application of the CB1 antagonist AM251 to aBNST (Supplementary Figure S3), 15 min before fear retrieval, prevented this shift towards sustained fear in the group that had received training with unpredictable CS-US pairings, whereas vehicle injection into aBNST had no effect (Figure 1b). Furthermore, phasic response profiles after predictable CS-US pairings prevailed after AM251 application (Figure 1b). Together, these results suggest that the eCB system contributes to the shift from phasic to sustained components of conditioned fear via CB1 receptors in aBNST.

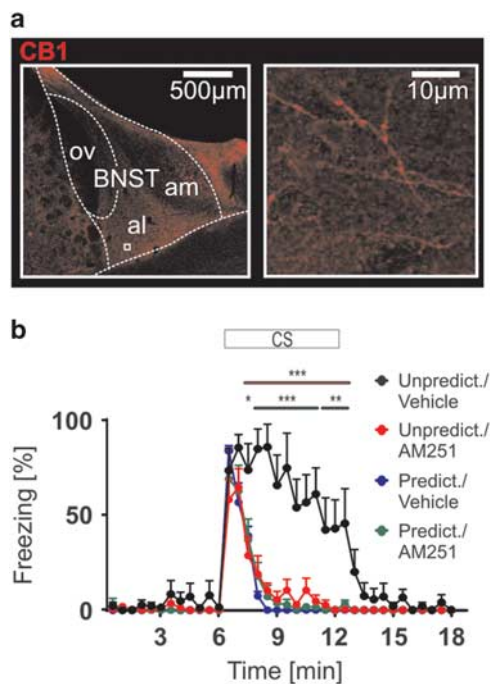


**Figure 1.** Pattern of CB1 expression in anterodorsal BNST (adBNST) and shift from sustained to phasic fear after pharmacological blockade of CB1. **(a)** Regional distribution of CB1 in the BNST, with immunopositive fiber-like elements in alBNST (magnified region as indicated). **(b)** Conditioned fear after local application of AM251 into adBNST in unpredictable- (red symbols;  $N=9$ ) and predictable-group (green symbols;  $N=5$ ), compared with vehicle injection in unpredictable-group (black symbols;  $N=5$ ) and predictable-group (blue symbols;  $N=5$ ). Note that sustained fear is prevented by AM251, whereas robust phasic fear responses prevail in both, unpredictable- and predictable-groups. Responses significantly differ between unpredictable/vehicle- and unpredictable/AM251-animals (group,  $F_{1,12}=37.06$ ;  $P<0.001$ ; group $\times$ time-interaction,  $F_{35,420}=8.909$ ;  $P<0.001$ ) as well as between unpredictable/vehicle- and predictable/AM251-group (group,  $F_{1,8}=29.96$ ;  $P<0.001$ ; group $\times$ time-interaction,  $F_{35,280}=7.054$ ;  $P<0.001$ ). No differences were observed between unpredictable/AM251- and predictable/AM251-, nor between predictable/vehicle- and predictable/AM251-group. For histological controls of injection sites see Supplementary Figure S2. All data obtained from C57BL/6J mice. (RM ANOVA; \*\*= $P<0.05$ , \*\*\*= $P<0.001$ , by *post hoc* Bonferroni).

Amygdala-BNST projections are considered fundamental in controlling phasic and sustained fear,<sup>11,17</sup> and CB1 receptors are located at presynaptic sites in BNST.<sup>29</sup> To functionally identify relevant amygdala inputs to BNST, we targeted channelrhodopsin-2 fused to enhanced yellow fluorescent protein (ChR2-eYFP) under the control of a synapsin promoter to distinct amygdalar regions (Supplementary Figure S4). After 5–7 weeks, ChR2-eYFP was observed in cell bodies of amygdala and fibers in BNST (Figures 2a, c and e). Cell bodies in BNST were devoid of ChR2-eYFP in all transduced animals ( $N=44$ ). In *ex vivo* BNST slices, labeled projection sites were visualized, single BNST neurons were electrophysiologically recorded and ChR2-eYFP-containing axon terminals were optically stimulated to provoke transmitter release, thereby evoking postsynaptic currents. The influence of the eCB system was assessed through established protocols of DSI and DSE synaptic transmission, to monitor retrograde eCB signaling via presynaptic CB1 receptors.<sup>26,29</sup> Targeting ChR2-eYFP to BA revealed projections predominantly to alBNST, and optical stimulation of ChR2-eYFP-containing terminals evoked excitatory postsynaptic currents (eEPSCs) sensitive to the AMPA receptor

antagonist DNQX in 10 out of 19 alBNST neurons (Figure 2a). All 10 neurons displayed significant DSE that was blocked by AM251 (10  $\mu\text{M}$  in the bathing solution; Figure 2b; statistical data in Supplementary Table S2). Targeting CeA revealed similar projections sites in alBNST, which, when light-stimulated, evoked inhibitory postsynaptic currents (eIPSCs). The eIPSCs were sensitive to the GABA<sub>A</sub> receptor antagonist gabazine (Figure 2c) and displayed significant CB1-mediated DSI (Figure 2d). Compared with DSE at BA inputs, DSI at CeA inputs was significantly larger in amplitude and longer in duration (Figure 2g). Medial amygdala (MeA) projected mostly to ambBNST, and gave rise to GABAergic eIPSCs not displaying DSI in any of the ambBNST neurons tested ( $N=10/5$ , Figures 2e–g). These results show a distinct pattern of CB1-mediated regulation of amygdala projections to BNST: BA and CeA inputs to alBNST are suppressed after activation of presynaptic CB1 receptors, whereas MeA inputs to ambBNST are not regulated via CB1 receptors. These conclusions are in line with previous data on CB1 receptor localization and function in BNST<sup>38</sup> and the regional pattern of CB1 immunoreactivity (Figure 1a).

Next, we sought to identify the nature of BNST target neurons receiving CB1-regulated amygdalar inputs. AAV-ChR2-eYFP was targeted to amygdala in GAD67-eGFP mice, allowing recording from visually identified putative GABAergic and non-GABAergic neurons. Stimulation of BA projections evoked eEPSCs in all tested eGFP-negative alBNST neurons, all of which displayed DSE (Figure 3a), whereas BA-evoked synaptic responses were not observed in any of the recorded eGFP-positive neurons in alBNST. CeA projections gave rise to eIPSCs in both eGFP-positive and eGFP-negative neurons in alBNST, of which only eGFP-negative ones displayed DSI (Figure 3b). Finally, we used local electrical stimulation to evoke postsynaptic currents in alBNST neurons and to probe CB1-mediated modulation irrespective of specific afferent inputs. Data are illustrated in Figures 3c and d and show that both DSI and DSE exist in both eGFP-negative and eGFP-positive neurons in alBNST. These results suggest that eGFP-negative (putative non-GABAergic) neurons in alBNST receive BA glutamatergic and CeA GABAergic afferent inputs that are regulated by the eCB system via presynaptic CB1 receptors. eGFP-positive (putative GABAergic) neurons in alBNST receive GABAergic inputs from CeA not underlying CB1 modulation and seem to miss inputs from BA.

To assess the behavioral impact of CB1 receptors on amygdala-alBNST connections, we used mice holding a loxP-flanked transcriptional stop-cassette upstream of the CB1-coding region, which prevents CB1 expression (Stop-CB1<sup>39</sup>), and targeted AAV-Cre-ChR2-eYFP to BA/CeA to locally rescue CB1 expression (Stop-CB1+AAV-Cre). Immunostainings confirmed the lack of CB1 in Stop-CB1 mice ( $N=2$ ; Figure 4a). In Stop-CB1 mice after AAV-Cre injections, CB1 immunoreactivity was observed in BA/CeA and on fiber-like structures forming immunopositive mesh-like patterns in alBNST, indicating the rescue of CB1 receptors ( $N=4$ ; Figure 4b). Furthermore, optical stimulation of ChR2-containing terminals *ex vivo* evoked eEPSCs and eIPSCs in alBNST target neurons displaying DSE and DSI, respectively, indicating the functional rescue of CB1 receptors in amygdala-BNST projections in Stop-CB1+AAV-Cre mice (Figure 4c). Recordings in sections of Stop-CB1-mice did not yield DSE or DSI in alBNST (Figure 4c). Next, mice were fear-conditioned using the paradigm with unpredictable CS–US pairings proven to evoke sustained fear.<sup>13</sup> Stop-CB1 mice displayed rapidly declining phasic freezing during CS presentation (Figure 4d), not significantly different from that observed during pharmacological blockade of CB1 receptors with AM251 in adBNST of C57BL/6J mice during CS presentation (Figure 1b; statistical data in Supplementary Table S1). Mice with bilateral local rescue of CB1 (Stop-CB1+AAV-Cre; Supplementary Figure S5) displayed sustained fear (Figure 4d), which was significantly different from the phasic profile in Stop-CB1 and indistinguishable from the sustained profile in vehicle injected C57BL/6J mice



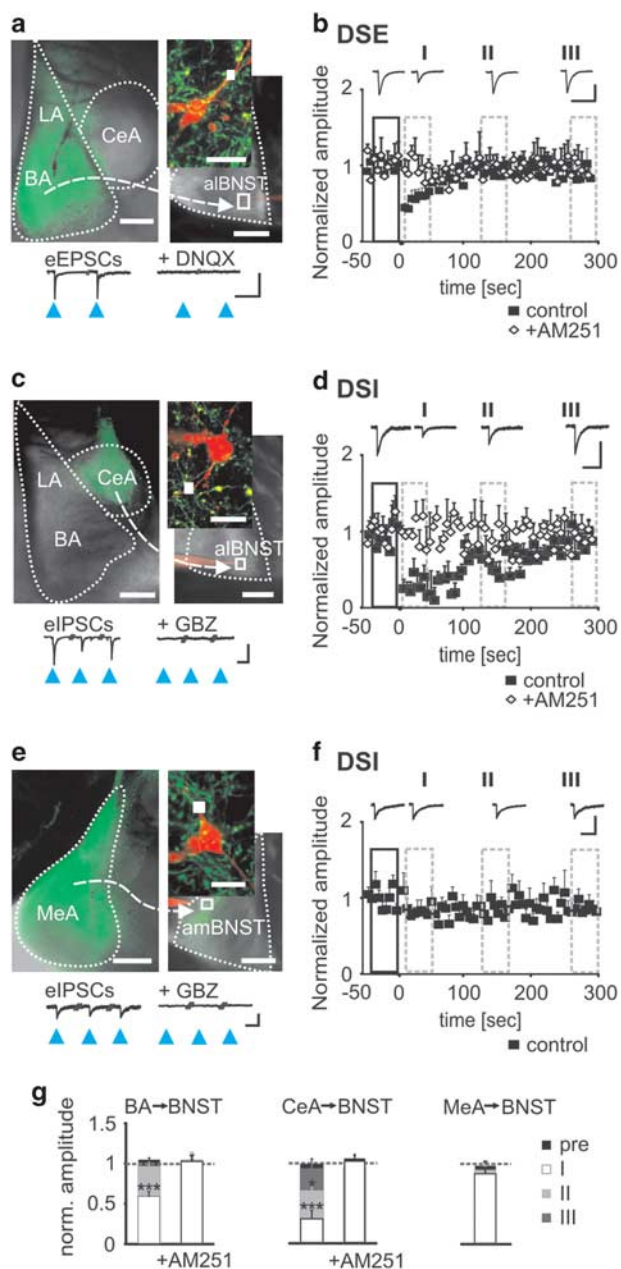


**Figure 2.** CB1-mediated suppression of excitatory (DSE) and inhibitory (DSI) synaptic transmission in distinct amygdala projections to alBNST. **(a, c, e)** Injection sites, projection area and recorded single BNST neurons (Alexa-Fluor594-filled patch pipette) for BA **(a)**, CeA **(c)**, and MeA **(e)** ChR2-eYFP injections. (Scale bars 200  $\mu$ m, 10  $\mu$ m). Note eYFP-labeled neuropil in BNST, indicating amygdala projection fibers. White squares near recorded neurons indicate optical stimulation areas, evoking excitatory postsynaptic currents (eEPSCs) (original traces exemplified) blocked by DNQX at putative BA inputs **(a)**, and eIPSCs blocked by gabazine (GBZ) at putative CeA and MeA inputs **(c, e)**. For further details see Supplementary Figure S1. **(b, d, f)** DSE and DSI at distinct inputs to BNST neurons. Averaged normalized eEPSC **(b)** and evoked inhibitory postsynaptic currents (eIPSC) **(d, f)** amplitudes, before and after postsynaptic depolarization (–60 to 0 mV; 10 s duration; at times zero). Original traces depicted immediately before and after (I), and at ~130 s (II) and ~270 s (III) after the postsynaptic depolarization. **(g)** Summary bar graph showing the magnitude of suppression at the three different projections, at the three time points after depolarization marked in **b, d, f**. Note suppression of eEPSCs at putative BA **(b, g; N = 10/5; F<sub>3,27</sub> = 13.9; P < 0.001)** and of eIPSCs at putative CeA inputs **(d, g; N = 9/6; F<sub>3,24</sub> = 23.7; P < 0.001)**, lack of suppression at putative MeA inputs **(f, g; N = 10/5)**, and sensitivity to AM251 (open diamonds; **b, g; N = 5/4; c, g; N = 8/6**). Repeated-measures ANOVA detected significant effect of time ( $F_{68,1156} = 5.3, P < 0.001$ ) and significant group  $\times$  time-interaction ( $F_{1,17} = 13.6, P < 0.01$ ) between DSE BA terminals and DSI CeA terminals. Amplitudes were significantly different between DSE BA terminals and DSI CeA terminals at time point I ( $P < 0.05$ ; one-sample *t*-test) and time point II ( $P < 0.01$ ; one-sample *t*-test). All data obtained from C57BL/6J mice (RM ANOVA, \* =  $P < 0.05$ , \*\*\* =  $P < 0.001$ , by *post hoc* Bonferroni; scale bars 50 ms and 50 pA).

Figure S6). Next, we targeted AAV-Cre to BA/CeA of mice where two loxP sites flanked the CB1-coding region (CB1-flx<sup>41</sup>) to delete CB1 receptors in BA/CeA (CB1-flx+AAV-Cre), which resulted in phasic freezing during CS presentation (Figure 4f), similar to that found after genetic depletion of CB1 in Stop-CB1 (Figure 4d) and significantly different from that in wild-type like CB1-flx mice (Figure 4f).

As both CeA GABAergic and BA glutamatergic inputs to alBNST were found to be regulated by CB1 receptors, we sought to dissect their contribution to fear sustainment by using Stop-CB1 mice with cell-type-specific rescue of CB1 in glutamatergic (Glu-CB1-RS) or GABAergic neurons (GABA-CB1-RS). In alBNST neurons, DSE and DSI occurred in Glu-CB1-RS and GABA-CB1-RS, respectively, confirming cell-type-specific CB1 rescue (Figure 5a). After training with unpredictable CS–US pairings, both GABA-CB1-RS and Glu-CB1-RS mice displayed conditioned freezing with an intermediate temporal profile between phasic and sustained fear (Figures 5b and c). Next, AAV-Cre was targeted to BA in GABA-CB1-RS, to rescue CB1 in BA glutamatergic pathways. Similarly in Glu-CB1-RS, AAV-Cre was targeted to CeA, to rescue CB1 in CeA GABAergic pathways. In both groups of animals, the typical sustained fear phenotype was reinstated (Figures 5b and c). These results suggest that stimulation of CB1 receptors on BA and CeA inputs to alBNST, likely mediated via glutamatergic and GABAergic synaptic connections, is necessary and sufficient for sustained fear to unpredictable threat stimuli, whereas these CB1 receptors are not involved in phasic fear to a predictable threat.

## DISCUSSION

The present study provides evidence that CB1 receptors on distinct amygdala inputs to alBNST determine the fear profile in response to predictable versus unpredictable threat. The fear training paradigm is based on a protocol described in a rat study by Walker and Davis<sup>40</sup> and has been adopted for application in mice.<sup>13</sup> In these protocols, auditory stimuli are paired with US in a

(Figure 1b; statistical data in Supplementary Table S1). These results suggest that local rescue of CB1 receptors in BA/CeA reinstated sustained fear, although they do not allow us to distinguish between influences of CB1 on various targets of efferent amygdala projections. To identify the impact of CB1 receptors in BNST, we bilaterally injected AM251 in adBNST in Stop-CB1 mice in which CB1 had been locally rescued (Stop-CB1 +AAV-Cre+AM251; Figure 4e and Supplementary Figures S5 or S6a). This intervention prevented sustained fear, in that only phasic freezing occurred in response to CS presentation (Figure 4e), undistinguishable from responses seen during absence (Stop-CB1; Figure 4d) or pharmacological blockade of CB1 receptors (Figure 1b; statistical data in Supplementary Table S1). Application of AM251 outside the adBNST had no such effect (Supplementary Figure S6). In Stop-CB1 in which amygdala had been injected with empty AAV, lacking the Cre-coding region, the phasic-type of fear response prevailed (Supplementary

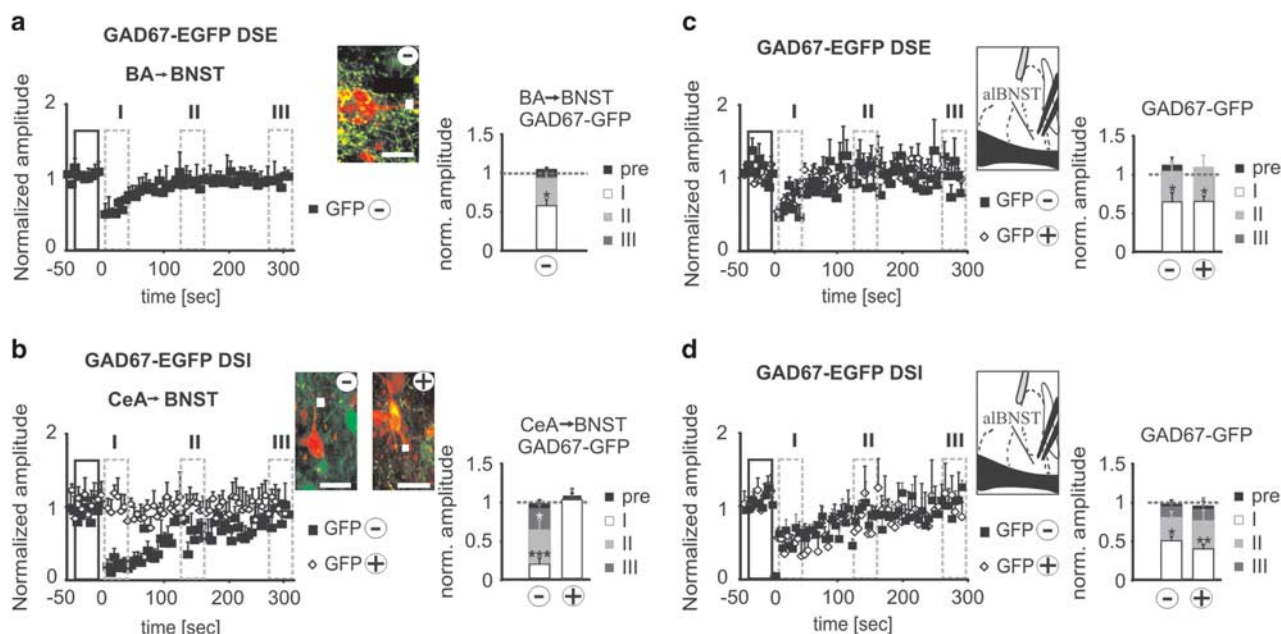


**Figure 3.** Input-specific DSE and DSI in distinct types of alBNST neurons. **(a, b)** Light-evoked EPSCs **(a)** and IPSCs **(b)** recorded in GFP-negative (–; closed symbols) and GFP-positive (+; open symbols) alBNST neurons (examples illustrated in insets, scale bar 10  $\mu$ m), after targeting Chr2-eYFP to BA **(a)** and CeA **(b)** in GAD67-eGFP mice. Note occurrence of DSE and DSI at putative BA ( $N = 7/4$ ;  $F_{3,18} = 10.1$ ;  $P < 0.001$ ) and CeA inputs, respectively ( $N = 7/4$ ;  $F_{3,18} = 16.7$ ;  $P < 0.001$ ) to GFP-negative alBNST neurons, and lack of DSI in GFP-positive cells ( $N = 7/4$ ). **(c, d)** EPSCs **(c)** and IPSCs **(d)** evoked by local electrical stimulation (position of stimulation electrode illustrated in insets) recorded in GFP-negative (–; closed symbols) and GFP-positive (+; open symbols) alBNST neurons. Note occurrence of both DSE and DSI in both GFP-negative (DSE:  $N = 5/3$ ;  $F_{3,12} = 5.1$ ;  $P < 0.05$ ; DSI:  $N = 5/2$ ;  $F_{3,12} = 7.8$ ;  $P < 0.01$ ) and GFP-positive alBNST neurons (DSE:  $N = 6/3$ ;  $F_{3,15} = 6.3$ ;  $P < 0.05$ ; DSI:  $N = 8/4$ ;  $F_{3,21} = 6.4$ ;  $P < 0.01$ ) **(c)**. Summary bar graphs show the magnitude of suppression in the respective types of neurons and stimulation arrangement, at three time points (I–III; for details see Figure 2). (RM ANOVA, \* =  $P < 0.05$ , \*\* =  $P < 0.01$ , \*\*\* =  $P < 0.001$ , by *post hoc* Bonferroni).

temporally predictable or unpredictable fashion, and during the recall test fear is measured within seconds (phasic fear) and minutes (sustained fear) of long duration CS presentation (reviewed in ref. 11). Although fear sustainment critically depends on unpredictability of CS–US pairings,<sup>11,13</sup> diminishing threat probability contributes to the rapid decline in phasic fear responses after training with predictable CS–US pairings.<sup>14</sup> A number of previous studies have demonstrated that phasic and sustained components of fear are pharmacologically dissociable<sup>42</sup> and involve distinct regions of the extended amygdala.<sup>17,43</sup> Our results indicate that CB1 receptors on distinct amygdala inputs to non-GABAergic neurons in alBNST are both necessary and sufficient for the shift from phasic- to sustained-type of fear responses. Using molecular inactivation and rescue techniques, we revealed the importance of these projections for regulation of these behaviors, and, we allocated the function of a defined protein, the presynaptic CB1 receptor, to these projections. We defined this protein function to be necessary by using a loss-of-function approach, that is, specific inactivation of CB1 receptors in these projections. In view of substantial interpretational limitations of this approach (see ref. 44), we advanced our study to the next step, by defining the sufficient function of CB1 receptors in these projections for sustained fear. In a mouse line lacking CB1 receptors, we reconstituted CB1 receptor function in distinct amygdala–BNST pathways to rescue the behavioral phenotype, and tested the behavioral significance of the reconstituted CB1 receptors in the BNST through local pharmacological intervention. Conceptually, by implementing the rescue experiments, we were able to adhere to the rigorous genetic approach commonly used in advanced genetic models, including *Drosophila*, yeast and *C. elegans*. To date, this approach

has rarely been implemented into the genetic dissection of mouse brain function.<sup>45–47</sup>

Both CeA GABAergic and BA glutamatergic inputs to alBNST were found to be regulated by CB1. Interfering with these two input pathways separately, through cell-type-specific (GABAergic versus glutamatergic) rescue approaches, resulted in a time course of fear responses intermediate between phasic and sustained. As a corollary, the two input pathways to alBNST seem to cooperate in determining the individual fear response profile. This is in line with the CB1 expression at both GABAergic and glutamatergic axon terminals, and the exclusive presynaptic nature of CB1 receptors in BNST.<sup>29,38</sup> In BNST neurons (both projection neurons and interneurons), the endocannabinoid system mediates short-term suppression (that is, DSE or DSI) via 2-AG acting on presynaptic CB1 receptors, whereas long-term depression (that is, LTD) of excitatory inputs is mediated via anandamide acting on postsynaptic TRPV1 receptors.<sup>29</sup> This pre- and postsynaptic segregation of proteins underlying short-term suppression and long-term depression, respectively, in BNST would exclude a contribution of LTD-like processes at excitatory inputs to the CB1-mediated effects on fear response profiles described in the present study. Of note, endocannabinoid-mediated long-term depression has been found to involve presynaptic CB1 receptors in other synaptic pathways, such as GABAergic synaptic inputs to basolateral amygdala (BLA) neurons.<sup>25</sup> Assuming a similar scenario in BNST, combined CB1-mediated DSI and LTD at CeA inputs would result in a long-term decrease in GABAergic influence and thence tonic disinhibition of target neurons in alBNST. Majority of BNST neurons are GABAergic/peptidergic and minority are glutamatergic, although their distinctive properties and projection sites remain to be determined in detail.<sup>48–51</sup> CB1-modulated amygdala inputs target non-GABAergic alBNST neurons, thus putative



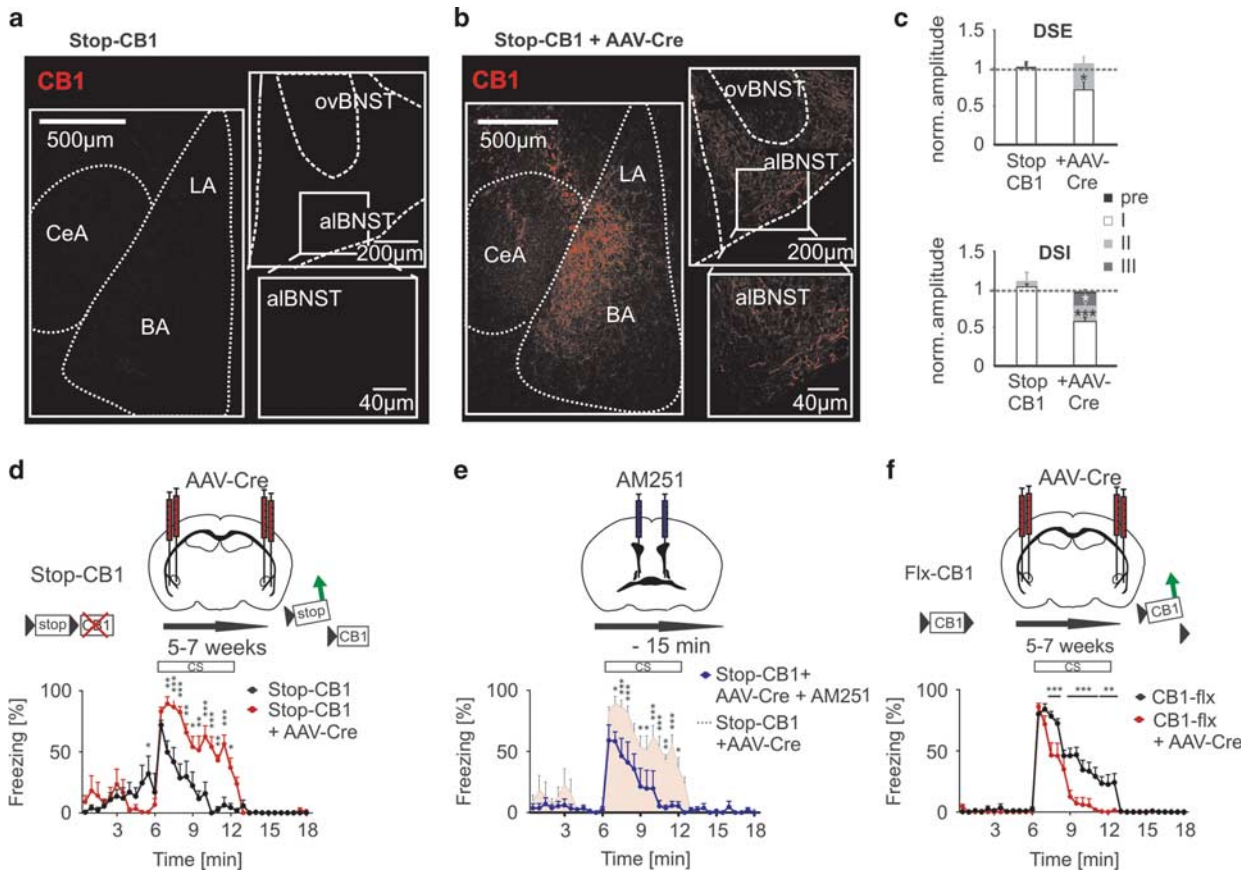


**Figure 4.** Rescue of CB1 in amygdala-BNST projections: functional specificity and sufficiency for sustained fear responses. **(a, b)** CB1 immunostaining indicating lack of CB1 in amygdala and anterolateral BNST (alBNST) in Stop-CB1 mice **(a)**, and expression of CB1 in BA/CeA and fiber-like elements in alBNST after targeting AAV-Cre to BA/CeA in Stop-CB1 **(b)**; magnified regions as indicated. **(c)** Summary bar graphs of DSE (upper) and DSI (lower) in light-evoked PSCs at BA and CeA inputs to alBNST neurons, respectively. Note lack of suppression in Stop-CB1 (DSE:  $N = 6/3$ ; DSI:  $N = 8/3$ ), and re-instatement of DSE ( $N = 6/3$ ;  $F_{3,15} = 12.5$ ;  $P < 0.01$ ) and DSI ( $N = 9/4$ ;  $F_{3,24} = 19.4$ ;  $P < 0.001$ ) after targeting AAV-Cre to BA/CeA. (RM ANOVA,  $* = P < 0.05$ ,  $*** = P < 0.001$ , by *post hoc* Bonferroni *t*-test). **(d, e)** Conditioned fear upon CS presentation (mean freezing, % of 30 s time bins) after training with unpredictable CS-US pairings. Note phasic-type of response in Stop-CB1 **(d)**,  $N = 6$ , black symbols), and the shift to sustained responses after targeting AAV-Cre to BA/CeA and resulting rescue of CB1 **(d)**, Stop-CB1+AAV-Cre,  $N = 5$ ; red symbols) (RM ANOVA: group,  $F_{1,9} = 7.179$ ;  $P = 0.0252$ ; group  $\times$  time-interaction,  $F_{35,315} = 7.192$ ;  $P < 0.001$ ;  $* = P < 0.05$ ,  $** = P < 0.01$ ,  $*** = P < 0.001$ , *post hoc* Bonferroni), and prevention of this shift by local application of AM251 to adBNST in Stop-CB1+AAV-Cre, 15 min before fear retrieval **(e)**,  $N = 5$ ; blue symbols, dashed line indicates sustained responses after targeting AAV-Cre to BA/CeA in Stop-CB1 animals from panel **d**) (RM ANOVA: group,  $F_{1,8} = 13.97$ ;  $P = 0.0057$ ; group  $\times$  time-interaction,  $F_{35,280} = 4.258$ ;  $P < 0.001$ ;  $* = P < 0.05$ ,  $** = P < 0.01$ ,  $*** = P < 0.001$ , *post hoc* Bonferroni). **(f)** Conditioned fear in CB1-flx ( $N = 11$ , black symbols), shifting to more phasic response types after targeting AAV-Cre to BA/CeA and resulting in loss of CB1 **(f)**, CB1-flx+AAV-Cre,  $N = 7$ , red symbols) (RM ANOVA: group,  $F_{1,16} = 12.17$ ;  $P = 0.003$ ; group  $\times$  time-interaction,  $F_{35,560} = 6.868$ ;  $P < 0.001$ ;  $* = P < 0.05$ ,  $** = P < 0.01$ ,  $*** = P < 0.001$ , by *post hoc* Bonferroni).

glutamatergic neurons. In ventral BNST, glutamatergic projection neurons display enhanced activity in response to aversive stimuli, associated with anxiogenic behavioral phenotypes, whereas firing rates of GABAergic neurons are depressed.<sup>23</sup> Assuming similar cell-type-specific functional divergence in alBNST, CB1 receptors seem to control afferent inputs to fear-provoking neurons. Fear-on neurons in CeA generate tonic barrages of spikes, compared with phasic spike patterns in BA neurons in response to fear-conditioned stimuli,<sup>21,22</sup> suggesting a rapid excitatory and strong tonic inhibitory influence on alBNST target neurons. In the present study, separate populations of alBNST non-GABAergic neurons were tested for the presence of DSE or DSI at BA and CeA inputs. Failures of CB1-mediated suppression of synaptic transmission were not detected in any of the tested cells, suggesting that BA and CeA projections converge onto single alBNST neurons and are both regulated via presynaptic CB1 receptors. This suggests a scenario, where BA glutamatergic inputs evoke postsynaptic depolarization of alBNST target neurons, subsequent production of endocannabinoids (most likely 2-arachidonoyl glycerol, 2-AG)

and stimulation of presynaptic CB1 receptors at both BA glutamatergic and CeA GABAergic inputs, which results in short-term suppression of glutamate and GABA release at the respective inputs.<sup>52</sup> The activity and sensitivity profiles of CB1 receptors are typically higher at GABAergic compared with glutamatergic connections.<sup>26,39</sup> This effect and CB1-mediated long-term depression at GABAergic inputs, as discussed above, suggest that CB1-mediated depression of GABAergic CeA inputs results in tonic disinhibition and evolvement of slow activation in alBNST target neurons (Figure 5d). In keeping with this, sustained fear during recall after training with unpredictable CS-US pairings is associated with a transient reduction in spike firing followed by slow onset activity, likely representing the tonic disinhibitory influence.<sup>24</sup> By comparison, alBNST neurons display a rather heterogeneous spectrum of responses to discrete fear-conditioned stimuli.<sup>20</sup> Although the exact types of amygdalar input and alBNST target neurons remain to be determined, the present results let us conclude that CB1-mediated regulation of distinct CeA and BA inputs to non-GABAergic neurons in alBNST is

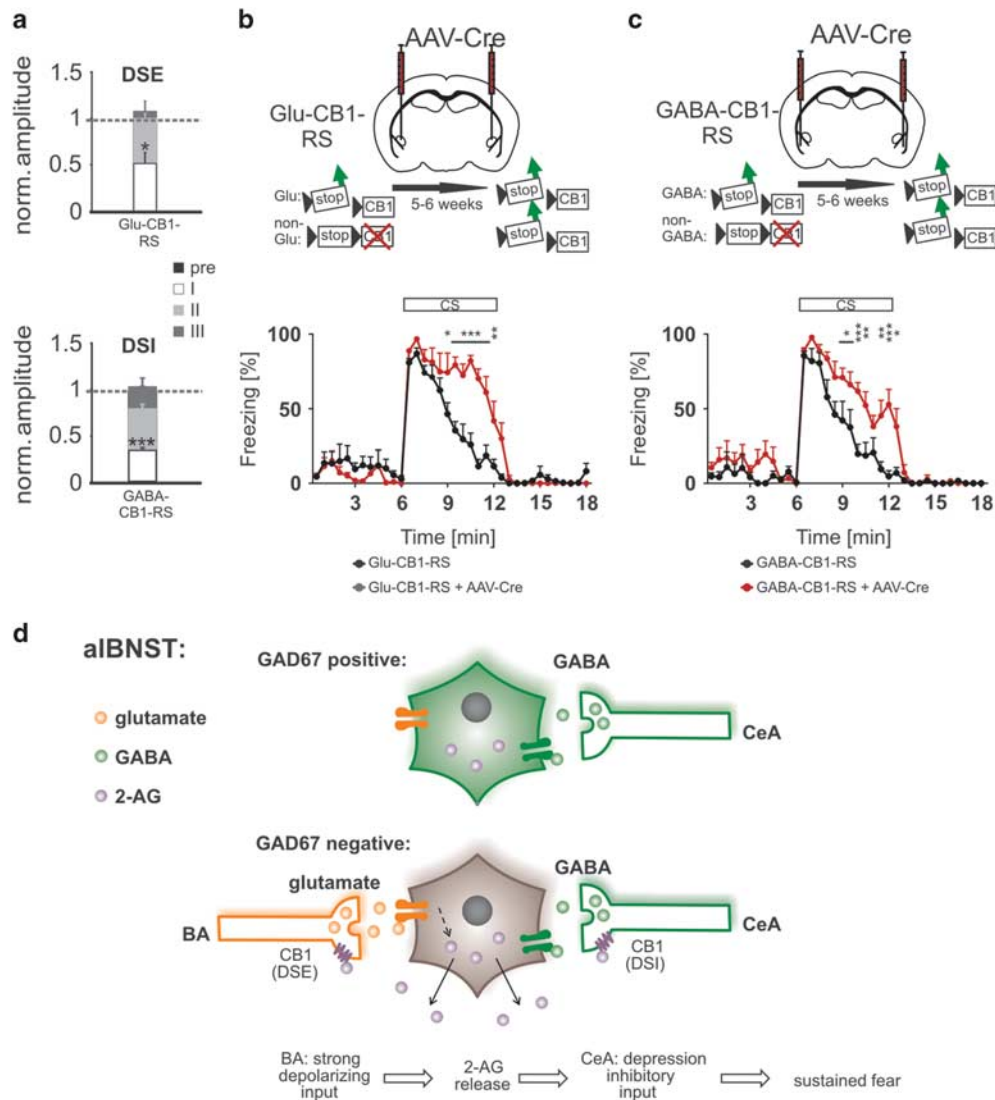


**Figure 5.** (a–c) Cell-type-specific rescue of CB1 receptors in amygdala-BNST projections. Crossing Stop-CB1 mice with mice expressing Cre recombinase under control of cell-type-specific regulatory elements (Dlx-Cre, NEX-Cre) yielded offspring with rescued CB1 receptor expression in forebrain GABAergic neurons (GABA-CB1-RS; **a**) and dorsal telencephalic glutamatergic neurons (Glu-CB1-RS, **b**), respectively. (a) Summary bar graphs of DSE (upper) and DSI (lower) in light-evoked EPSCs at BA and IPSCs at CeA inputs to anterolateral BNST (alBNST) neurons of Glu-CB1-RS (upper panel) and GABA-CB1-RS (lower panel). For details, see the legend of Figure 2. Note DSE at putative BA terminals in Glu-CB1-RS (top;  $N = 6/3$ ;  $F_{3,15} = 13.9$   $P < 0.001$ ) and DSI of eIPSCs at putative CeA inputs in GABA-CB1-RS (bottom;  $N = 8/4$ ;  $F_{3,21} = 20.5$   $P < 0.001$ ), (RM ANOVA,  $* = P < 0.05$ ,  $** = P < 0.01$ ,  $*** = P < 0.001$ , by Bonferroni *post hoc* test). (b, c; lower panels) Conditioned fear-on CS presentation (mean freezing, % of 30 s time bins) after training with unpredictable CS–US pairings. Both GABA-CB1-RS (**c**; black symbols;  $N = 6$ ) and Glu-CB1-RS (**b**, black symbols;  $N = 7$ ) displayed freezing responses that declined during CS presentation, but were significantly different from the phasic-like response in Stop-CB1 and the sustained response profile in C57BL/6J. Targeting AAV-Cre to BA in GABA-CB1-RS (**c**; red symbols;  $N = 6$ ) and to CeA in Glu-CB1-RS (**b**; red symbols;  $N = 7$ ) to locally rescue CB1 in glutamatergic and GABAergic neurons, respectively, resulted in a significant sustenance of CS-evoked freezing in both groups (RM ANOVA, group,  $F_{1,10} = 10.03$ ;  $P < 0.01$ ; group  $\times$  time-interaction,  $F_{35,350} = 3.294$  for GABA-CB1-RS;  $P < 0.001$ ; group,  $F_{1,12} = 12.53$ ;  $P < 0.0041$ ; group  $\times$  time-interaction,  $F_{35,420} = 5.938$ ;  $P < 0.001$  for Glu-CB1-RS;  $* = P < 0.05$ ,  $** = P < 0.01$ ,  $*** = P < 0.001$ , by *post hoc* Bonferroni *t*-test). (d) Schematic illustration of CB1 receptor-regulated pathways from BA and CeA to alBNST, and their proposed contribution to fear sustenance. In GAD67 positive neurons (upper scheme), GABAergic inputs from CeA are devoid of CB1 receptors and inputs from BA could not be detected. In GAD67 negative neurons (lower scheme), CB1 receptors are expressed at glutamatergic BA inputs and GABAergic CeA inputs. Activity at BA inputs evokes postsynaptic depolarization of alBNST target neurons, subsequent production of endocannabinoid 2-arachidonoyl glycerol (2-AG), stimulation of presynaptic CB1 receptors at both BA and CeA inputs, and short-term suppression of glutamate (DSE) and GABA (DSI) release at the respective inputs. Given the high activity profile of CB1 receptors at GABAergic connections, this results in tonic disinhibition and slow activation in alBNST target neurons, mediating sustenance of fear responses.

causal for the temporal evolution of the phasic-sustained fear response profile during predictable and unpredictable threat. Human imaging studies indeed demonstrated that a forebrain region corresponding to the rodent BNST is activated during

unpredictable threat in healthy subjects.<sup>4</sup> Although the amygdala is responsive to the onset of cues signaling the unpredictable occurrence of a potential threat, the BNST in concert with other brain areas is involved in sustained anxiety in humans.<sup>53</sup>

Furthermore, BNST is activated during threat anticipation in spider phobics.<sup>54</sup> Although fearful responses to a nonspecific stressor were found analogous between clinically anxious patients and controls, sustained fear to unpredictable aversive stimuli distinguished individuals with posttraumatic stress or panic disorder from controls and individuals with generalized anxiety disorder,<sup>11</sup> corroborating the role of unpredictability in anxiety disorders. The present study identifies specific neuronal pathways from amygdala to BNST, and reveals activity-dependent regulation of a distinct subset of these synaptic connections by the endocannabinoid system. This regulation, in turn, is both necessary and sufficient for determining the shift from phasic to prolonged states of fear, reminiscent of anxiety symptoms in humans. Whether or not blockade of CB1 receptors is a feasible concept for interfering with the development of prolonged states of fear or anxiety remains to be addressed in future studies.

### CONFLICT OF INTEREST

The authors declare no conflict of interest.

### ACKNOWLEDGMENTS

The authors thank Julia Schröder, Elke Naß, Birgit Herrenpöth, and Svetlana Kiesling, Anisa Kosan and Andrea Conrad for excellent technical assistance, and Annika Lüttjohann, Michael Döngi and Peter Blässe for helpful advice. The project was funded by the German research foundation (CRC-TRR58, TPA03 to H.C.P., and TPA04 to B.L. and H.C.P.).

### REFERENCES

- Sylvers P, Lilienfeld SO, LaPrairie JL. Differences between trait fear and trait anxiety: implications for psychopathology. *Clin Psychol Rev* 2011; **31**: 122–137.
- Grupe DW, Nitschke JB. Uncertainty and anticipation in anxiety: an integrated neurobiological and psychological perspective. *Nat Rev Neurosci* 2013; **14**: 488–501.
- Avery SN, Clauss JA, Blackford JU. The human BNST: functional role in anxiety and addiction. *Neuropsychopharmacology* 2015; **41**: 126–141.
- Alvarez RP, Chen G, Bodurka J, Kaplan R, Grillon C. Phasic and sustained fear in humans elicits distinct patterns of brain activity. *Neuroimage* 2011; **55**: 389–400.
- Pape H-C, Paré D. Plastic synaptic networks of the amygdala for the acquisition, expression, and extinction of conditioned fear. *Physiol Rev* 2010; **90**: 419–463.
- Ehrlich I, Humeau Y, Grenier F, Ciochi S, Herry C, Lüthi A. Amygdala inhibitory circuits and the control of fear memory. *Neuron* 2009; **62**: 757–771.
- Johansen JP. Neuroscience: anxiety is the sum of its parts. *Nature* 2013; **496**: 174–175.
- Duvarci S, Paré D. Amygdala microcircuits controlling learned fear. *Neuron* 2014; **82**: 966–980.
- Maren S, Quirk GJ. Neuronal signalling of fear memory. *Nat Rev Neurosci* 2004; **5**: 844–852.
- Tovote P, Fadok JP, Lüthi A. Neuronal circuits for fear and anxiety. *Nat Rev Neurosci* 2015; **16**: 317–331.
- Davis M, Walker DL, Miles L, Grillon C. Phasic vs sustained fear in rats and humans: role of the extended amygdala in fear vs anxiety. *Neuropsychopharmacology* 2010; **35**: 105–135.
- Grillon C, Baas JP, Lissek S, Smith K, Milstein J. Anxious responses to predictable and unpredictable aversive events. *Behav Neurosci* 2004; **118**: 916–924.
- Daldrup T, Remmes J, Lesting J, Gaburro S, Fendt M, Meuth P *et al*. Expression of freezing and fear-potentiated startle during sustained fear in mice. *Genes Brain Behav* 2015; **14**: 281–291.
- Seidenbecher T, Remmes J, Daldrup T, Lesting J, Pape H-C. Distinct state anxiety after predictable and unpredictable fear training in mice. *Behav Brain Res* 2016; **304**: 20–23.
- Foa EB, Zinbarg R, Rothbaum BO. Uncontrollability and unpredictability in post-traumatic stress disorder: an animal model. *Psychol Bull* 1992; **112**: 218–238.
- Mineka S, Kihlstrom JF. Unpredictable and uncontrollable events: a new perspective on experimental neurosis. *J Abnorm Psychol* 1978; **87**: 256–271.
- Walker DL, Miles LA, Davis M. Selective participation of the bed nucleus of the stria terminalis and CRF in sustained anxiety-like versus phasic fear-like responses. *Prog Neuropsychopharmacol Biol Psychiatry* 2009; **33**: 1291–1308.
- Davis M, Walker DL, Lee Y. Amygdala and bed nucleus of the stria terminalis: differential roles in fear and anxiety measured with the acoustic startle reflex. *Philos Trans R Soc Lond B Biol Sci* 1997; **352**: 1675–1687.
- Kim S-Y, Adhikari A, Lee SY, Marshel JH, Kim CK, Mallory CS *et al*. Diverging neural pathways assemble a behavioural state from separable features in anxiety. *Nature* 2013; **496**: 219–223.
- Haufler D, Nagy FZ, Paré D. Neuronal correlates of fear conditioning in the bed nucleus of the stria terminalis. *Learn Mem* 2013; **20**: 633–641.
- Ciochi S, Herry C, Grenier F, Wolff SBE, Letzkus JJ, Vlachos I *et al*. Encoding of conditioned fear in central amygdala inhibitory circuits. *Nature* 2010; **468**: 277–282.
- Herry C, Ciochi S, Senn V, Demmou L, Müller C, Lüthi A. Switching on and off fear by distinct neuronal circuits. *Nature* 2008; **454**: 600–606.
- Jennings JH, Sparta DR, Stamatakis AM, Ung RL, Pleil KE, Kash TL *et al*. Distinct extended amygdala circuits for divergent motivational states. *Nature* 2013; **496**: 224–228.
- Daldrup T, Lesting J, Meuth P, Seidenbecher T, Pape H-C. Neuronal correlates of sustained fear in the anterolateral part of the bed nucleus of stria terminalis. *Neurobiol Learn Mem* 2016; **131**: 137–146.
- Azad SC, Monory K, Marsicano G, Cravatt BF, Lutz B, Zieglängsberger W *et al*. Circuitry for associative plasticity in the amygdala involves endocannabinoid signaling. *J Neurosci* 2004; **24**: 9953–9961.
- Castillo PE, Younts TJ, Chávez AE, Hashimoto Y. Endocannabinoid signaling and synaptic function. *Neuron* 2012; **76**: 70–81.
- Kamprath K, Romo-Parra H, Häring M, Gaburro S, Doengi M, Lutz B *et al*. Short-term adaptation of conditioned fear responses through endocannabinoid signaling in the central amygdala. *Neuropsychopharmacology* 2011; **36**: 652–663.
- Marsicano G, Wotjak CT, Azad SC, Bisogno T, Rammes G, Cascio MG *et al*. The endogenous cannabinoid system controls extinction of aversive memories. *Nature* 2002; **418**: 530–534.
- Puente N, Cui Y, Lassalle O, Lafourcade M, Georges F, Venance L *et al*. Polymodal activation of the endocannabinoid system in the extended amygdala. *Nat Neurosci* 2011; **14**: 1542–1547.
- Ramkise TS, Nyilas R, Bluett RJ, Gamble-George JC, Hartley ND, Mackie K *et al*. Multiple mechanistically distinct modes of endocannabinoid mobilization at central amygdala glutamatergic synapses. *Neuron* 2014; **81**: 1111–1125.
- Riebe CJ, Wotjak CT. Endocannabinoids and stress. *Stress* 2011; **14**: 384–397.
- Morena M, Patel S, Bains JS, Hill MN. Neurobiological interactions between stress and the endocannabinoid system. *Neuropsychopharmacology* 2015; **41**: 80–102.
- Hill MN, Patel S, Campolongo P, Tasker JG, Wotjak CT, Bains JS. Functional interactions between stress and the endocannabinoid system: from synaptic signaling to behavioral output. *J Neurosci* 2010; **30**: 14980–14986.
- Lutz B, Marsicano G, Maldonado R, Hillard CJ. The endocannabinoid system in guarding against fear, anxiety and stress. *Nat Rev Neurosci* 2015; **16**: 705–718.
- Guggenhuber S, Monory K, Lutz B, Klugmann M. AAV vector-mediated over-expression of CB1 cannabinoid receptor in pyramidal neurons of the hippocampus protects against seizure-induced excitotoxicity. *PLoS One* 2010; **5**: e15707.
- Jüngling K, Lange MD, Szuklarek HJ, Lesting J, Erdmann FS, Doengi M *et al*. Increased GABAergic efficacy of central amygdala projections to neuropeptide S neurons in the brainstem during fear memory retrieval. *Neuropsychopharmacology* 2015; **40**: 2753–2763.
- Lange MD, Jüngling K, Paulukat L, Vieler M, Gaburro S, Sosulina L *et al*. Glutamic acid decarboxylase 65: a link between GABAergic synaptic plasticity in the lateral amygdala and conditioned fear generalization. *Neuropsychopharmacology* 2014; **39**: 2211–2220.
- Puente N, Elezgarai I, Lafourcade M, Reguero L, Marsicano G, Georges F *et al*. Localization and function of the cannabinoid CB1 receptor in the anterolateral bed nucleus of the stria terminalis. *PLoS One* 2010; **5**: e8869.
- Ruehle S, Remmers F, Romo-Parra H, Massa F, Wickert M, Wörtge S *et al*. Cannabinoid CB1 receptor in dorsal telencephalic glutamatergic neurons: distinctive sufficiency for hippocampus-dependent and amygdala-dependent synaptic and behavioral functions. *J Neurosci* 2013; **33**: 10264–10277.
- Walker DL, Davis M. Role of the extended amygdala in short-duration versus sustained fear: a tribute to Dr. Lennart Heimer. *Brain Struct Funct* 2008; **213**: 29–42.
- Marsicano G, Goodenough S, Monory K, Hermann H, Eder M, Cannich A *et al*. CB1 cannabinoid receptors and on-demand defense against excitotoxicity. *Science* 2003; **302**: 84–88.
- Miles L, Davis M, Walker D. Phasic and sustained fear are pharmacologically dissociable in rats. *Neuropsychopharmacology* 2011; **36**: 1563–1574.
- Walker DL, Toufexis DJ, Davis M. Role of the bed nucleus of the stria terminalis versus the amygdala in fear, stress, and anxiety. *Eur J Pharmacol* 2003; **463**: 199–216.
- Alger BE. Not too excited? Thank your endocannabinoids. *Neuron* 2006; **51**: 393–395.



- 45 Balthasar N, Dalggaard LT, Lee CE, Yu J, Funahashi H, Williams T *et al*. Divergence of melanocortin pathways in the control of food intake and energy expenditure. *Cell* 2005; **123**: 493–505.
- 46 Soria-Gómez E, Bellocchio L, Reguero L, Lepousez G, Martin C, Bendahmane M *et al*. The endocannabinoid system controls food intake via olfactory processes. *Nat Neurosci* 2014; **17**: 407–415.
- 47 Higa KK, Ji B, Buell MR, Risbrough VB, Powell SB, Young JW *et al*. Restoration of Sp4 in forebrain GABAergic neurons rescues hypersensitivity to ketamine in Sp4 hypomorphic mice. *Int J Neuropsychopharmacol* 2015; **18**: pyv063.
- 48 Hammack SE, Mania I, Rainnie DG. Differential expression of intrinsic membrane currents in defined cell types of the anterolateral bed nucleus of the stria terminalis. *J Neurophysiol* 2007; **98**: 638–656.
- 49 Hazra R, Guo J-D, Ryan SJ, Jasnow AM, Dabrowska J, Rainnie DG. A transcriptomic analysis of type I-III neurons in the bed nucleus of the stria terminalis. *Mol Cell Neurosci* 2011; **46**: 699–709.
- 50 Rodríguez-Sierra OE, Turesson HK, Paré D. Contrasting distribution of physiological cell types in different regions of the bed nucleus of the stria terminalis. *J Neurophysiol* 2013; **110**: 2037–2049.
- 51 Kudo T, Uchigashima M, Miyazaki T, Konno K, Yamasaki M, Yanagawa Y *et al*. Three types of neurochemical projection from the bed nucleus of the stria terminalis to the ventral tegmental area in adult mice. *J Neurosci* 2012; **32**: 18035–18046.
- 52 Chevalyere V, Castillo PE. Heterosynaptic LTD of hippocampal GABAergic synapses: a novel role of endocannabinoids in regulating excitability. *Neuron* 2003; **38**: 461–472.
- 53 Herrmann MJ, Boehme S, Becker MPI, Tupak S V, Guhn A, Schmidt B *et al*. Phasic and sustained brain responses in the amygdala and the bed nucleus of the stria terminalis during threat anticipation. *Hum Brain Mapp* 2015; **37**: 1091–1102.
- 54 Straube T, Mentzel H-J, Miltner WHR. Waiting for spiders: brain activation during anticipatory anxiety in spider phobics. *Neuroimage* 2007; **37**: 1427–1436.

Supplementary Information accompanies the paper on the *Molecular Psychiatry* website (<http://www.nature.com/mp>)